Technical Notes

TECHNICAL NOTES are short manuscripts describing new developments or important results of a preliminary nature. These Notes cannot exceed six manuscript pages and three figures; a page of text may be substituted for a figure and vice versa. After informal review by the editors, they may be published within a few months of the date of receipt. Style requirements are the same as for regular contributions (see inside back cover).

Gas Permeability of Oblique-Layered Carbon-Cloth Ablator

Toshiyuki Suzuki* and Keisuke Sawada†
Tohoku University, Sendai 980-8579, Japan
and
Tetsuya Yamada‡ and Yoshifumi Inatani§
Institute of Space and Astronautical Science, Sagamihara 229-8510, Japan

Nomenclature

d = diameter of unsealed portion of test specimen, m
h = thickness of test specimen, m
p = pressure, Pa
v = volume, m^3
γ = permeability, m^2
$\tilde{\gamma}$ = normalized permeability
θ = ply angle of carbon cloth, deg
ρ = density, kg/m^3
μ = viscosity of air at room temperature, 1.82×10^{-5} Pa · s

Subscripts

c = char
v = virgin

Introduction

WHEN a cloth–layered carbon–phenolic ablator is heated in an arcjet wind tunnel, a delamination between layers sometimes occurs depending on the amount of heat input.[1] This is believed to occur when pressure force of pyrolysis gas exceeds a certain limit of bonding strength between layers. To avoid delamination, pyrolysis gas must be released properly through the char layer behind the pyrolysis zone, which is influenced either by the angle of cloth layers or by the permeability of char layers. Therefore, the ablative heatshield of MUSES-C that was developed in the Institute of Space and Astronautical Science (ISAS) employed a tilted layup of carbon cloth with respect to the surface. The angle of cloth layers was determined from experimental study.[1]

Computer codes such as the HBI method[2] or the SCMA code[3] determine thermal response of ablative heatshield by solving equations in one-dimensional space. This simplification is justified when radius of surface curvature is much larger than the thickness of ablator. This condition is amply satisfied for entry capsules hitherto flown into planetary atmospheres. For the analysis of delamination problem, however, it is certainly necessary to solve two-dimensional equations in which dependence of gas permeability on ply angle of carbon-cloth should be accounted for. It is also known that gas permeability of ablative materials depends on a volume of char in the test piece (hereafter referred to char volume). In this study, the gas permeability of carbon-cloth ablator developed in ISAS is determined experimentally in terms of char volume with varying ply angle.

Experimental Configuration

For permeability measurement, test specimens with various char volume and ply angle are first prepared. The test specimens are circular disks made of carbon–phenolic with a diameter of 12 mm and a thickness of 2.5 mm. The test specimens are weighed on an electronic balance (Shimazu, AEG-220), placed in a temperature-controlled oven and then exposed to the following temperature cycle: 1) Test specimens are exposed at 100°C for 1 h to remove moisture content, 2) then cooled to room temperature and weighed, 3) exposed at temperature $T = 300 \sim 800$°C for 3 h in argon atmosphere, and 4) cooled to room temperature and weighed again to obtain mass loss and char volume. The heat up rate is approximately 20°C/min. The obtained char volume data are summarized in Table 1, in which the mass of the specimen at the end of 3 h exposure is designated as final mass.

When all specimens are prepared, the permeability of the test specimen is measured one after another. Figure 1 shows a schematic of experimental apparatus. In this experiment, high-pressure air reservoired in sampling tube 1 flows through the porous test specimen fixed in two ducts. The two ducts can be connected by means of flanges made of stainless steel. The left duct is connected both to the sampling tube 1 (1000 ml) and to a pressure transducer (Kyowa,

Table 1 Char volume and ply angle of test specimens

Ply angle θ, deg	Dry mass, g	Exposure temperature, °C	Final mass, g	Char volume v_c
0	0.3811	300	0.3499	0.331
0	0.3812	350	0.3358	0.480
0	0.3794	400	0.3182	0.660
0	0.3800	450	0.3059	0.794
0	0.3810	500	0.2998	0.861
0	0.3824	800	0.2867	1.0
90	0.3832	300	0.3524	0.335
90	0.3830	350	0.3379	0.492
90	0.3842	400	0.3245	0.643
90	0.3855	450	0.3118	0.782
90	0.3817	500	0.3017	0.885
90	0.3915	800	0.2913	1.0
5	0.3767	800	0.2881	1.0
22.5	0.3766	800	0.2882	1.0
45	0.3665	800	0.2819	1.0
60	0.3673	800	0.2838	1.0
80	0.3650	800	0.2803	1.0

Presented as Paper 2003-4045 at the AIAA 36th Thermophysics Conference, Hilton Walt Disney World, Orlando, FL, 23–26 June 2003; received 3 November 2003; revision received 9 February 2004; accepted for publication 9 February 2004.

*Graduate Student, Department of Aeronautics and Space Engineering; Aobayama 01; suzuki@cfd.mech.tohoku.ac.jp; currently Invited Researcher, Institute of Space Technology and Aeronautics, 7-44-1 Jindaiji Higashi-machi, Chofu; suzuki.toshiyuki@jaxa.jp. Student Member AIAA.

†Professor, Department of Aeronautics and Space Engineering, Aobayama 01. Associate Fellow AIAA.

‡Research Associate, Department of Aeronautics and Space Engineering, 3-1-1 Yoshinodai.

§Professor, Department of Aeronautics and Space Engineering, 3-1-1 Yoshinodai. Senior Member AIAA.

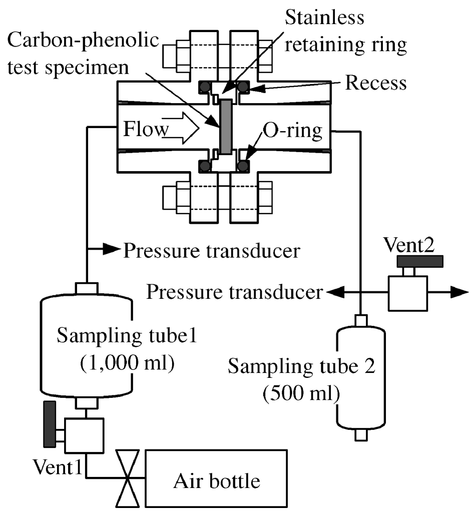

Fig. 1 Schematic of experimental apparatus.

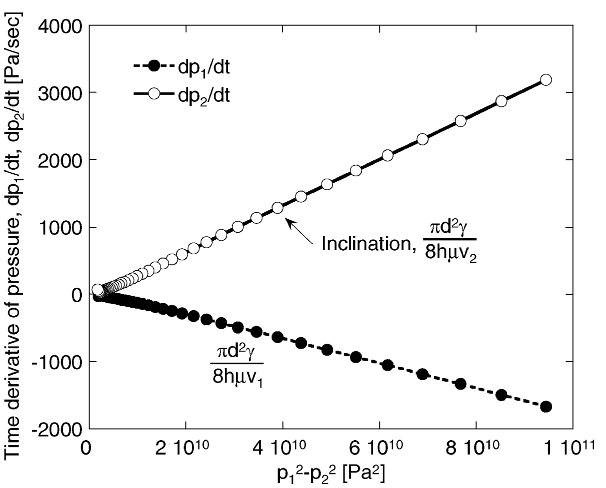

Fig. 2 Typical example of pressure data obtained in the present experiment.

PHF-S-5MPSA2). This sampling tube is further connected to an air bottle through vent 1. The right duct is also connected to a sampling tube 2 (500 ml) and to a pressure transducer (Kyowa, PHF-S-2MPSA2). The test specimen embedded in a stainless retaining ring is pinched between the right and left flanges. The gap between the test specimen and the retaining ring is sealed by epoxy-type bond (AREMCO, 805). The diameter of the unsealed portion of the test specimen is kept as much as possible to 10 mm.

Each test is performed as follows. The test specimen fixed to the retaining ring is placed on the left flange. The right flange is placed on the top of the left flange. The junction of two flanges is secured by using 6 bolts. Next, the sampling tube 1 is filled by air at either 0.3 or 1.0 MPa (absolute) while the both vents are kept opened. The sampling tube 2 is maintained at atmospheric pressure. After the vents are closed, the variations of the pressure are recorded as a function of time. Every test is performed at room temperature. With the assumption that the flow can be described by Darcy's law, the permeability of test piece is determined by solving the following equations using the pressure histories obtained in this experiment[4,5]:

$$\frac{\partial p_2}{\partial t} = \frac{\pi d^2 \gamma}{8 h \mu v_2}\left(p_1^2 - p_2^2\right) \tag{1}$$

$$\frac{\partial p_1}{\partial t} = -\frac{v_2}{v_1}\frac{\partial p_2}{\partial t} \tag{2}$$

Results

A typical example of the pressure data obtained in this experiment is shown in Fig. 2. One can see that the time derivative of p_2 is mostly in proportion to $p_1^2 - p_2^2$. Therefore, the permeability of the test specimen can be determined from the inclination of the fitted straight line using the least-squares method. The obtained permeability is shown in Fig. 3 as a function of char volume,

$$v_c = (\rho_v - \rho)/(\rho_v - \rho_c) \tag{3}$$

In this study, the measured permeability varies from about 10^{-17} to 10^{-13} m^2 as the char volume varies from 0.3 to 1.0. Moreover, the permeability for the case of 90-deg ply angle is about three times larger than that for the case of the 0-deg ply angle. Possible errors in the present measurement are evaluated, where an examination is made of the uncertainty of the unsealed area and the machining accuracy of the test piece. The overall error in the permeability is determined within ±6%.

Figure 4 shows the normalized permeability as a function of ply angle for the case of $v_c = 1.0$. Because the ply angles of 0 and 90 deg coincide with that of the principal directions of carbon cloths, the permeability for the case of ply angle of $\theta (0 \le \theta \le 90$ deg) can be evaluated geometrically by the following equation:

$$\tilde{\gamma} = \tilde{\gamma}_{\theta=90}\sin^2\theta + \tilde{\gamma}_{\theta=0}\cos^2\theta \tag{4}$$

The fitted curve is in Fig. 4. As can be seen, the agreement is fairly good.

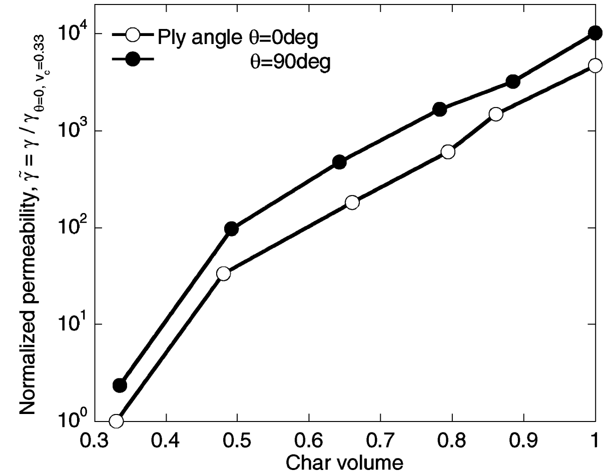

Fig. 3 Normalized permeability of carbon–phenolic ablator as a function of char volume.

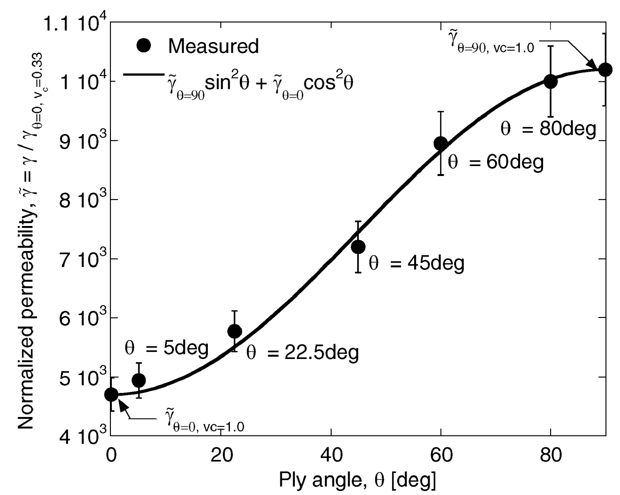

Fig. 4 Normalized permeability of carbon–phenolic ablator as a function of ply angle, v_c = 1.00.

Summary

In this study, the gas permeability of carbon-cloth ablator developed in ISAS is determined experimentally. The measured permeability varies for more than three orders of magnitude as the char volume varies from 0.3 to 1.0. The dependence of gas permeability on ply angle of the carbon cloth is also examined. The permeability for the case of 90-deg ply angle is about three times larger than that for the case of 0-deg ply angle. It is also shown that the variation of the measured permeability in terms of ply angle can be fitted fairly well with the curve determined by Eq. (4). In the study of delamination problem, thermal response of ablative test piece should be solved at least in two-dimensional space. The dependence of gas permeability on ply angle that is measured in this study will be used in such studies.

References

[1]Yamada, T., Ishii, N., Inatani, Y., and Honda, M., "Thermal Protection System of the Reentry Capsule with Superorbital Velocity," Inst. of Space and Astronautical Science, Rept. SP No. 17, Sagamihara, Japan, March 2003, pp. 245–261.

[2]Potts, R. L., "Application of Integral Methods to Ablation Charring Erosion, A Review," *Journal of Spacecraft and Rockets*, Vol. 32, No. 2, 1995, pp. 200–209.

[3]Ahn, H.-K., Park, C., and Sawada, K., "Response of Heatshield Material at Stagnation Point of Pioneer-Venus Probe," *Journal of Thermophysics and Heat Transfer*, Vol. 16, No. 3, 2002, pp. 432–439.

[4]McManus, H. L., "High-Temperature Thermochemical Behavior of Carbon–Phenolic and Carbon–Carbon Composites," Ph.D. Dissertation, Dept. of Mechanical Engineering, Stanford Univ., Stanford, CA, 1990.

[5]McManus, H. L., and Springer, G. S., "High Temperature Thermochemical Behavior of Carbon–Phenolic and Carbon–Carbon Composites, II. Results," *Journal of Composite Materials*, Vol. 26, No. 2, 1992, pp. 230–255.

Vibrational Population Enhancement in Nonequilibrium Dissociating Hypersonic Nozzle Flows

Eswar Josyula*
U.S. Air Force Research Laboratory,
Wright–Patterson Air Force Base, Ohio 45433
and
William F. Bailey†
U.S. Air Force Institute of Technology,
Wright–Patterson Air Force Base, Ohio 45433

Nomenclature

K_{eq} = equilibrium constant
k_f = dissociation-rate coefficient
k_r = recombination-rate coefficient
p = pressure
T = translational temperature
T_v = vibrational temperature
α_O = mass fraction of atomic oxygen
Θ_d = characteristic temperature of dissociation
ρ = total density
ρ_i = state density in the ith vibrational level
ρ_n = state density in the nth vibrational level
φ_n = depletion factor for state n, deviation of quasisteady distribution from equilibrium Boltzmann $\rho_n = \rho_n^o(1 + \varphi_n)$

Presented as Paper 2003-3778 at the AIAA 36th Thermophysics Conference, Orlando, FL, 23 June 2003; received 27 January 2004; revision received 3 May 2004; accepted for publication 3 May 2004.

*Research Aerospace Engineer, AFRL/VAAC, 2210 Eighth Street. Associate Fellow AIAA.

†Associate Professor, AFIT/ENP, 2950 Hobson Way.

Introduction

THE proper treatment of energy transfer between nonequilibrium molecular energy modes and dissociation has important implications in the accurate prediction of the aerothermodynamics of gas systems, namely, aerodynamic heating on hypersonic vehicles and thrust in propulsive nozzles.[1] At high temperatures, molecular collisions result in the exchange of the translational, rotational, vibrational, and electronic energies of the collision partners. The probabilities or effective cross sections of these elementary processes differ significantly, giving rise to widely separate relaxation times for the internal modes. Thus it becomes important to account for the rates of relaxation processes to predict the nonequilibrium behavior of these kinds of flows. Vibrational equilibration involves widely separated relaxation times ranging between the very short times for translational/rotational equilibration and the longer times for chemical and ionization equilibration. The disparate eigenvalues have significant physical and computational implications. Nonequilibrium vibrational energy distributions are required for prediction of dissociation rates, interpretation of radiation experiments, and interpretation of ionic recombination rates.

The effect of vibrational population depletion in dissociating flows behind shock waves for hypersonic applications was presented in the work of Josyula and Bailey.[2] The collisional approach to dissociation was adapted to model the nonequilibrium flow physics in the study of the dissociation kinetics of hypersonic flow past a blunt body. In this study, the vibrational master equations were coupled to fluid dynamic equations, and vibration-translation (V-T) process were considered in evaluating the vibrational population depletion effects of dissociation from the last quantum level. The role of the V-T process in the dissociation kinetics was delineated by assessing the competition between the V-T process, which primarily restores equilibrium, and the dissociation process, which perturbs the equilibrium state. The extent of the population depletion and the consequent reduction of the dissociation rates is sensitive to the temperature regime in the flowfield. For the dissociation kinetics of the nitrogen molecule, in the temperature range of 5000–15,000 K the new vibration-dissociation model yielded a substantial rate reduction relative to Park's equilibrium rate. The nonequilibrium conditions behind the shock wave of a blunt body exemplify the case where the translational temperature is greater than the vibrational temperature ($T > T_v$), ultimately approaching near-equilibrium conditions close to the surface of the body. The higher rate of dissociation vs recombination in blunt-body flows makes the vibrational population depletion effect significant in the vibration-dissociation coupling model.

In expanding nozzle flows, however, the effect of vibration-dissociation coupling on the vibrational population density is reversed and the population is enhanced. The sonic flow at the throat of the nozzle is in thermal equilibrium, and as the flow proceeds towards the exit of the nozzle the flow departs from the equilibrium conditions. The vibrational temperature freezes near the throat, and the translation temperature rapidly falls as a result of the expansion process. The flow exhibits higher degrees of nonequilibrium as it proceeds towards the exit. As the translational temperature starts dropping, the dissociation rate drops significantly. However for the same translational temperature drop, the change in the recombination rate is small, and the recombination rate remains consistently higher than the dissociation rate throughout most of the nozzle flowfield. This recombination-dominant flow leads to a population enhancement in the vibrational manifold under the nonequilibrium reactive conditions. A vibration-dissociation coupling model, thus, has to account for this enhancement to accurately predict the nonequilibrium chemistry. The role of the vibrational population enhancement in the development of vibration-dissociation coupling model in high-temperature nozzle flows in hypersonic applications is the objective of the present study.

The nonequilibrium vibrational energy distribution was modeled by the master equations to calculate the population distributions by